JOURNAL OF COMPUTATIONAL PHYSICS **136,** 272–288 (1997)
ARTICLE NO. CP975730

A Numerical Method Using Upwind Schemes for the Resolution of Two-Phase Flows

F. Coquel,*,[1] K. El Amine,*,†,[2] E. Godlewski,*,[1] B. Perthame,*,[1] and P. Rascle†,[2]

*Laboratoire d'Analyse Numérique-Tour 55-65 5ème étage, Université Pierre et Marie Curie, 4 place Jussieu, 75252 Paris cedex 05, France; †E.D.F./D.E.R./R.N.E./Ph.R., 1 avenue du Général de Gaulle, 92141 Clamart Cedex, France

Received April 9, 1996; revised December 18, 1996

This work is devoted to the numerical approximation of two-fluid flow models described by six balance equations. We introduce an original splitting technique which is especially derived to allow a straightforward extension to various and detailed exchange source terms. When based on suitable kinetic upwind schemes, the whole scheme preserves the positivity of all the thermodynamic variables under a fairly unrestrictive CFL like condition. Several stiff numerical tests, including phase separation, are displayed in order to highlight the efficiency of the method we propose. © 1997 Academic Press

1. INTRODUCTION

An accurate prediction of two-phase flow phenomena is essential to safety analysis of nuclear reactors under off-normal or accident conditions. In general, the ability to predict these phenomena depends on the availability of mathematical models and experimental correlations. Among several two-phase flow models, there are two fundamentally different formulations of the macroscopic field equations for two-phase flow systems; namely the two-fluid model and the mixture model (see [8, 19]). Here we are interested in the two-fluid model. It is considered to be appropriate for the most general and detailed description of transient two-phase flows. In the two-fluid model, each phase is separately described in terms of two sets of conservation equations. The interaction terms between two phases appear in the basic equations as transfer terms across the interphases. Because the number of necessary closure relations are considerably higher for the two-fluid model than for the mixture model, much more detailed experimental data are necessary to develop satisfactory closure relations. However, sufficient experimental information for developing reliable closure relations for the two-fluid model is often not available. Therefore, the present state of the art in the two-phase flow instrumentation implies that considerable uncertainties exist in the closure relations for the two-fluid model. Despite these shortcomings, however, there are a number of situations where the two-fluid model is more advantageous (or even necessary in some cases) than the mixture model (see [8]). Also, many authors agree on the basic form of the model (Eqs. (2.1), below), although it lacks some physical properties. The derivation of additional terms has been widely studied.

A specific concern is that most models presently used in the large computer codes are based on governing equations having complex eigenvalues (Wallis model [23]), but complex characteristics are in general thought to cause ill-posedness of the numerical solutions. In order to make their models hyperbolic, some researchers introduce formulations for interfacial coupling between the two separated momentum equations, including space and time derivatives of phasic physical quantities (virtual mass term, interfacial pressure; see [2] and the references therein; [16, 21]). Hence, the correct formulation of the basic two-fluid equations and the appropriate closure relations have been discussed during the past and, up to now, there does not exist a commonly agreed approach.

Our objective in this paper is to develop a simple numerical method capable of predicting two-phase flow phenomena with reasonable accuracy, computational efficiency, and, following the persistent uncertainties in two-phase modeling, the implementation of new terms may be accomplished without changing the basic solution method. That is the reason why we only treat here the simplified system (2.1). It is solved numerically by using an upwind numerical scheme based on a finite volume method. The unknowns are the conservative variables and all the quantities are computed at the centers of the cells. In a work under progress, coupling terms between the phases are being addressed regarding their numerical treatment within the frame of the present method (phase exchanges, acceleration, friction terms, and also real fluids); see [1].

We propose a resolution approach for the two-fluid model which reduces the problem to classical gas dynamics. Then we use a Boltzmann scheme involving compactly

[1] E-mail: coquel@ann.jussieu.fr; godlewski@ann.jussieu.fr; perthame@ann.jussieu.fr.

[2] E-mail: Khalid.El-Amine@der.edfgdf.fr; Paul.Rascle@der.edfgdf.fr.

0021-9991/97 $25.00
Copyright © 1997 by Academic Press
All rights of reproduction in any form reserved.

supported equilibrium functions. This method was introduced at first by Perthame [12] for the resolution of compressible Euler equations. This approach ensures the positivity of the pressure and of the densities of each phase, as well as the control of the void fraction which must stay within the interval [0, 1]. The conservation of total mass, momentum, and energy is also preserved by this method. Several numerical tests assert the possibility of computing stiff phenomena with our algorithm. For example, we can compute a separation problem where fronts propagate and one of the two phases disappears locally. For further methods on diphasic computations, we also refer to [18, 20] and the recent extension of the work in [4].

The format of this paper is as follows. In the first section we present the continuous model. Then, we describe our numerical approach. In Section 4, some stability properties are proved and the last section is devoted to the illustration of the scheme on well-known test cases.

2. TWO-FLUID MODEL OF TWO-PHASE FLOW

The two-fluid model is formulated by considering each phase separately in terms of two sets of conservation equations governing the balance of mass, momentum, and energy of each phase. Since the macroscopic fields of one phase are not independent of the other phase, the interaction terms which couple the transport of mass, momentum and energy of each phase across the interphase appear in the field equations. The balance equations are complemented by the state equations for the two phases and by additional correlations for the right-hand side coupling terms. The equations contain more dependent variables compared with the number of equations. Therefore, additional assumptions are necessary in order to close the system of equations. The most common procedure (to close the system of equations) is to postulate equal local pressure values for the two phases.

The simplest macroscopic balance equations for the equal pressure one-dimensional two-fluid model can be written under the following form, which can be eventually supplemented with specific terms for practical applications:

$$\partial_t(\alpha_v\rho_v) + \partial_x(\alpha_v\rho_v u_v) = 0, \tag{2.1.a}$$

$$\partial_t(\alpha_l\rho_l) + \partial_x(\alpha_l\rho_l u_l) = 0, \tag{2.1.b}$$

$$\partial_t(\alpha_v\rho_v u_v) + \partial_x(\alpha_v\rho_v u_v^2 + \alpha_v p) - p\partial_x\alpha_v = (p_i - p)\partial_x\alpha_v + \alpha_v\rho_v g, \tag{2.1.c}$$

$$\partial_t(\alpha_l\rho_l u_l) + \partial_x(\alpha_l\rho_l u_l^2 + \alpha_l p) - p\partial_x\alpha_l = (p_i - p)\partial_x\alpha_l + \alpha_l\rho_l g, \tag{2.1.d}$$

$$\partial_t\left(\alpha_v\rho_v\left(e_v + \frac{u_v^2}{2}\right)\right) + \partial_x\left(\alpha_v\rho_v\left(e_v + \frac{p}{\rho_v} + \frac{u_v^2}{2}\right)u_v\right) + p\partial_t\alpha_v = \alpha_v\rho_v g u_v, \tag{2.1.e}$$

$$\partial_t\left(\alpha_l\rho_l\left(e_l + \frac{u_l^2}{2}\right)\right) + \partial_x\left(\alpha_l\rho_l\left(e_l + \frac{p}{\rho_l} + \frac{u_l^2}{2}\right)u_l\right) + p\partial_t\alpha_l = \alpha_l\rho_l g u_l, \tag{2.1.f}$$

$$\alpha_v + \alpha_l = 1. \tag{2.2}$$

This system of equations represents the balance equations for mass (2.1.a), (2.1.b), momentum (2.1.c), (2.1.d), and energy (2.1.e), (2.1.f) of the vapor and liquid phases. The variables appearing in the above equations have the following meanings (here we set $k = v, l$ for the vapor and liquid phases):

α_k = volume fraction of k-phase,
ρ_k = density of k-phase,
u_k = velocity of k-phase,
e_k = specific internal energy of k-phase,
p = common pressure to the two phases,
p_i = interface pressure,
g = gravity constant.

These equations have to be supplemented by two equations of state. The standard form of the equation of state for each phase is given by a function relating the density to the pressure and the internal energy

$$\rho_k = \rho_k(p_k, e_k). \tag{2.3}$$

In general, there exist no explicit expressions for the relationships in Eqs. (2.3). In practice, they are approached by various explicit forms. But the most general relation is simply a tabular form. From thermodynamic principles, one can use any pair of thermodynamic variables, for example: (p_k, h_k) or (p_k, s_k). Also, in the system of equations (2.1), the density for each phase is one of the conservative variables. Therefore, it is computationally easier to deal with relations under the form

$$p_k = p_k(\rho_k, e_k). \tag{2.4}$$

Since we suppose that the two phases are in pressure equilibrium, we have

$$p_v = p_l = p;$$

i.e.,

$$p = p_v(\rho_v, e_v) = p_l(\rho_l, e_l). \tag{2.5}$$

The interfacial pressure p_i needs a closure equation, the simplest of which is $p_i = p$ (see (3.29) below for another example of closure relation and references). We now have six equations for the six unknowns ($\alpha_k\rho_k$, $\alpha_k\rho_k u_k$, $\alpha_k\rho_k(e_k + u_k^2/2)$) with $k = v$ (vapor), $k = l$ (liquid) completed with the three algebraic relations (2.2) and (2.5) for α_k and p.

Notice that many simplifications are encountered in practice (see [19; 8, pp. 85–238]). For instance Sainsaulieu [16] and Toumi [21] assume that the liquid phase is incompressible with constant density ρ_l, while the vapor phase is assumed to be an ideal gas governed by the state function

$$p = (\gamma - 1)\rho_v e_v, \tag{2.6}$$

with a constant coefficient ($\gamma > 1$).

For simplicity in exposition here, we assume that both phases are described by an equation of state of ideal gas type

$$e_k = \frac{p}{(\gamma_k - 1)\rho_k}, \tag{2.7}$$

where γ_k is a constant and represents the ratio of specific heat capacities of the fluid k. Typical values for γ are $\gamma = 1.4$ for a diatomic gas, e.g. air, and $\gamma = 1.0005$ for the liquid. This is reasonable at least, in a first step, when the vapor phase is always present and imposes its compressibility to the liquid phase. Researches are in progress to improve these laws.

It is very difficult to solve numerically the system of Eqs. (2.1) as it stands. Indeed, for $p_i = p$ it is not a hyperbolic system, and even for physically relevant expressions of $(p - p_i)$ it is only conditionally hyperbolic. Hence instabilities can occur in some situations. Additional physical effects, that are not modeled here, counterbalance these instabilities. But their explicit form is not settled precisely and they can be added in each specific case. This is what we do in specific applications. But here we restrict ourselves to the common model (2.1). Nevertheless, the mathematical structure of this system gives some fundamental physical properties that we would like to keep at the numerical level. As far as stability is concerned we wish to keep nonnegative densities, temperatures, pressure, and the void fraction (i.e., $\alpha = \alpha_v$) within the interval [0, 1]. Even though we do not use it later, notice that this system is also endowed with two entropy inequalities (one for each phase). In the case $p_i = p$, and for a γ-law (2.7) these entropy inequalities write

$$\partial_t \alpha_k\rho_k S_k + \partial_x \alpha_k\rho_k u_k S_k \le 0, \quad S_k = \ln \frac{\rho_k^{\gamma_k}}{p}. \tag{2.8}$$

We expect that they play an essential role in the stability. But at this moment, we were not able to recover the corresponding entropy-in-cell inequalities (see [5, 7, 11]).

Concerning accuracy, a basic property we need is to be able to recover the classical finite-volume schemes when only one phase is present ($\alpha_v = 0$ or $\alpha_l = 0$). In particular we wish to treat the most difficult case where one of the phases disappears (see the first numerical test in Section 5), i.e. $\alpha_v = 0$ or $\alpha_l = 0$ locally.

3. NUMERICAL METHOD

3.1. *A Two-Step Approach*

We develop a new method based on a decomposition of the system. This method allows us to apply advanced numerical techniques that have been recently developed and successfully applied to single phase flows (or compressible Euler equations). Let us briefly outline the main steps of the method. Being given the state variables at time t^n (α^n, p^n, ρ_k^n, u_k^n) (or the computational variables (m_k^n, $m_k^n u_k^n$, E_k^n)), we proceed as follows.

Step 1 (Hydrodynamical step). (i) we solve two classical and decoupled hydrodynamical systems using usual approximate Riemann solver and (ii) we include the source term ($p_i\partial_x\alpha$). Each of these two problems in Step 1 are close to a quasi-1D nozzle problem, where α is similar to the section of the nozzle. After the first step, we know the quantities $m_k^{n+1/2} = \alpha_k^{n+1/2}\rho_k^{n+1/2}$, $m_k^{n+1/2}u_k^{n+1/2}$, $E_k^{n+1/2}$, and the pressure of the two phases are different, in general.

Step 2 (Restoring equality of pressures). We compute α_k^{n+1}, p^{n+1}, ρ_k^{n+1}, e_k^{n+1} in order to restore the equality of the pressures between the two phases.

We now describe in more detail these two steps and introduce related notations. To simplify, we set $p_i = p$, but later, the interfacial pressure (3.29) will be considered.

First step (*hydrodynamical step*). In the first step, we solve the two following systems, one for each phase k ($k = v, l$),

$$\begin{aligned} &\partial_t(m_k) + \partial_x(m_k u_k) = 0,\\ &\partial_t(m_k u_k) + \partial_x(m_k u_k^2 + \tilde{p}_k) = p_k\partial_x\alpha_k + \alpha_k\rho_k g,\\ &\partial_t(E_k) + \partial_x((E_k + \tilde{p}_k)u_k) = \alpha_k\rho_k g u_k, \end{aligned} \tag{3.1}$$

where

$$\begin{aligned} m_k &= \alpha_k\rho_k,\\ E_k &= \alpha_k\rho_k(e_k + u_k^2/2),\\ \tilde{p}_k &= \alpha_k p_k = (\gamma_k - 1)m_k e_k. \end{aligned}$$

The two systems will be discretized explicitly and then they may be solved independently because these are uncoupled.

These two systems can be written in the compact form

$$\frac{\partial U_k}{\partial t} + \frac{\partial F(U_k)}{\partial x} = H(U_k), \tag{3.2}$$

where the vector U_k is defined by $U_k^{\mathrm{T}} = (m_k, m_k u_k, E_k)$, $k = v, l$. In what follows, the terms due to gravity forces will be ignored. In practice (see Section 5), these are treated using an explicit scheme.

Second step (*restoring equality of pressures*). In the second step, we solve the two following coupled systems for $k = v, l$:

$$\begin{aligned} &\partial_t m_k = 0, \\ &\partial_t (m_k u_k) = 0, \\ &\partial_t E_k = -p\,\partial_t \alpha_k. \end{aligned} \tag{3.3}$$

Thus the method involves a splitting which reduces the resolution of the full system (2.1) to classical hydrodynamics (3.1) with source terms, and a rather simple problem (3.3).

3.2. *Discretization of the First Step*

Next we explain how to solve the first step (3.1), i.e., the system of equations

$$\frac{\partial U}{\partial t} + \frac{\partial F(U)}{\partial x} = H(U), \tag{3.4}$$

where

$U = (m, mu, E)^{\mathrm{T}}$ is the vector of conservative variables,
$F(U) = (mu, mu^2 + \tilde{p}, (E + \tilde{p})u)^{\mathrm{T}}$ is the flux vector,
$H(U) = (0, p\,\partial_x \alpha, 0)^{\mathrm{T}}$ is the source term.

and

$E = m(e + u^2/2)$,
$\tilde{p} = (\gamma - 1)me$.

We note that the system of Eqs. (3.4) is composed of two physically different parts. The first one (the left-hand side) is in conservative form, but the second (the right-hand side) is in nonconservative form. At this level we would like to mention that contact discontinuities can occur but the equations stay meaningful; and for the applications we have in mind, shock waves as in classical compressible flows are not of primary interest.

We will use a classical finite volume approach and discretize (3.4) in

$$U_j^{n+1} - U_j^n + \sigma(F_{j+1/2}^n - F_{j-1/2}^n) = \Delta t H_j^n. \tag{3.5}$$

In order to explain this, we begin by dividing the spatial domain into N cells denoted by $K_j =]x_{j-1/2}, x_{j+1/2}[$ called control volumes. By choosing a mesh width Δx, a time step Δt and $\sigma = \Delta t/\Delta x$ we have

$$\begin{aligned} x_{j-1/2} &= (j - 1/2)\Delta x, \qquad && j \in \mathbb{Z}, \\ t^n &= n\Delta t, && n \in \mathbb{Z}. \end{aligned}$$

For simplicity we take a uniform mesh with Δx constant, although the method we discuss can be extended to variable meshes.

Classically the finite volume method produces approximations U_j^n of the mean value of U on the cell $[x_{j-1/2}, x_{j+1/2}]$ at time t^n.

We assume that, at time t^n, we know U_j^n, an approximation to the average of the solution to (3.4) on the cell $]x_{j-1/2}, x_{j+1/2}[$; and we wish to calculate U_j^{n+1}, the mean value of an approximate solution at time $t^{n+1} = t^n + \Delta t$. We deduce (3.5) from (3.4), setting

$$U_j^n \simeq \frac{1}{\Delta x} \int_{x_{j-1/2}}^{x_{j+1/2}} U(x, t^n)\, dx, \tag{3.6}$$

$$F_{j+1/2}^n \simeq \frac{1}{\Delta t} \int_{t^n}^{t^{n+1}} F(U(x_{j+1/2}, t))\, dt, \tag{3.7}$$

$$H_j^n \simeq \frac{1}{\Delta t\, \Delta x} \int_{t^n}^{t^{n+1}} \int_{x_{j-1/2}}^{x_{j+1/2}} H(U(x,t))\, dx\, dt. \tag{3.8}$$

We now detail these approximations. We begin by the fluxes $F_{j+1/2}^n$. As is well known, the numerical fluxes $F_{j+1/2}^n$ can be obtained through approximate Riemann solvers (see Harten, Lax, and Van Leer [7]). In practice, we have tested the Roe solver [15] and a kinetic solver [12]. But for tests where one of the volume fractions can vanish, the kinetic method is preferred because of its better behavior (see also the positivity results stated in Theorem 1). By contrast the Roe solver is known to be unstable close to a vacuum, which means here $\alpha = 0$ or 1.

In the case of three-point schemes, these numerical fluxes have the form

$$F_{j+1/2}^n = F(U_j^n, U_{j+1}^n). \tag{3.9}$$

And for the sake of completeness, we describe the second scheme, namely the kinetic scheme. Consider the left-hand side of the system (3.4), i.e.,

$$\frac{\partial U}{\partial t} + \frac{\partial F(U)}{\partial x} = 0. \tag{3.10}$$

In order to describe the kinetic solver, we introduce the "equilibrium functions" associated with the state vector $U^n(x)$ which are defined by

$$f^n(x,v) = m^n(x)\sqrt{m^n(x)/\tilde{p}^n(x)}\,\chi\left((v-u^n(x))\sqrt{m^n(x)/\tilde{p}^n(x)}\right), \quad (3.11)$$

$$g^n(x,v) = \lambda m^n(x)\sqrt{\tilde{p}^n(x)/m^n(x)}\,\chi\left((v-u^n(x))\sqrt{m^n(x)/\tilde{p}^n(x)}\right), \quad (3.12)$$

with

$$\lambda = \frac{3-\gamma}{2(\gamma-1)}. \quad (3.13)$$

Here χ is a nonnegative even function that satisfies

$$\int_{\mathbb{R}} (1, w, w^2)\chi(w)\,dw = (1,0,1). \quad (3.14)$$

The simplest choice (we will use in practice) is due to [12]; it reads

$$\chi(w) = \frac{1}{2\sqrt{3}}\mathbf{1}_{|w|\le\sqrt{3}}. \quad (3.15)$$

But other choices are possible such as the physical Maxwellian $1/\sqrt{2\pi}\,\exp(-w^2/2)$. We refer to [5, 7] for more details on the motivations for introducing this method and other references.

We notice that the integration of the two functions defined above with respect to the v variable yields

$$m^n(x) = \int_{\mathbb{R}} f^n(x,v)\,dv, \quad (3.16)$$

$$m^n u^n(x) = \int_{\mathbb{R}} v f^n(x,v)\,dv, \quad (3.17)$$

$$E^n(x) = \int_{\mathbb{R}} \left(\frac{v^2}{2} f^n(x,v) + g^n(x,v)\right) dv, \quad (3.18)$$

and, instead of solving the system of Eqs. (3.10) we solve the two following linear transport equations

$$\begin{cases} \partial_t f + v\partial_x f = 0 \\ f(x,v,t^n) = f^n(x,v) \end{cases} \text{ and } \begin{cases} \partial_t g + v\partial_x g = 0 \\ g(x,v,t^n) = g^n(x,v) \end{cases} \quad (3.19)$$

with $t \ge t^n$, $(x, v) \in R^2$.

The following lemma is at the basis of the Boltzmann schemes (Perthame [12]).

LEMMA 1. *Let Δt be a small time step and $t \in [t^n, t^n + \Delta t]$. The quantities*

$$\begin{aligned} m(x,t) &= \int_{\mathbb{R}} f(x,v,t)\,dv, \\ mu(x,t) &= \int_{\mathbb{R}} v f(x,v,t)\,dv, \\ E(x,t) &= \int_{\mathbb{R}} \left(\frac{v^2}{2} f(x,v,t) + g(x,v,t)\right) dv \end{aligned} \quad (3.20)$$

are first order in Δt approximations of the solutions to (3.10).

Next assume that $U^n(x)$ is piecewise constant:

$$U^n(x) = U_j^n = (m_j^n, m_j^n u_j^n, E_j^n) \quad \text{for } x \in]x_{j-1/2}\cdot x_{j+1/2}[. \quad (3.21)$$

In the finite volume approach, once the numerical flux functions $F_{j+1/2}$ in (3.7) which approximate the physical fluxes at the interface between the cells j and $j+1$ are known, the formula for updating the cell averages of the conserved quantities corresponding to (3.10) is

$$U_j^{n+1} = U_j^n - \frac{\Delta t}{\Delta x}(F_{j+1/2}^n - F_{j-1/2}^n). \quad (3.22)$$

Assume the CFL condition (for the choice 3.15):

$$\Delta t \le \Delta x/(|u^n(x)| + \sqrt{3}\sqrt{\tilde{p}^n(x)/m^n(x)}) \quad \forall x \in \mathbb{R}. \quad (3.23)$$

By using (3.20) and the condition (3.23), the integration of (3.10) gives the flux $F_{j+1/2}^n$ (a three entries vector) which is written

$$F_{j+1/2}^n = F^+(U_j^n) + F^-(U_{j+1}^n), \quad (3.24)$$

with

$$F^+(U_j) = \int_{w \ge -u_j\sqrt{m_j/\tilde{p}_j}} \begin{pmatrix} (u_j + w\sqrt{\tilde{p}_j/m_j}) \\ (u_j + w\sqrt{\tilde{p}_j/m_j})^2 \\ (u_j + w\sqrt{\tilde{p}_j/m_j})^3/2 + \dfrac{\lambda\tilde{p}_j}{m_j}(u_j + w\sqrt{\tilde{p}_j/m_j}) \end{pmatrix} m_j\chi(w)\,dw. \quad (3.25)$$

Here we have generically denoted

$$U = (m, mu, E)^{\mathrm{T}}. \quad (3.26)$$

The flux F^- is obtained by replacing "$\ge$" by "$\le$" in

the above integrals. As is proved in [12], this scheme is consistent for any function χ which satisfies (3.14).

We now describe the discretization of the term $H(U) = (0, p\partial\alpha/\partial x, 0)^{\mathrm{T}}$. This term plays an essential role in the stability of the global scheme. We will treat it wisely and, thus, following the nature of physical phenomena and the characteristics of the conservation law system (i.e., hyperbolic ($p_i \neq p$) or not ($p_i = p$)). We could have used a two fractional step-method which consists of integrating the left part of the system (3.1) in a first step and the right one in a second step. This method has been used for the nozzle problem by several authors. For reasons we will see later, we have preferred to integrate the two parts in a single step.

We propose to discretize the term $\partial_x\alpha$ in the expression $p\partial_x\alpha$ (or $p_i\partial_x\alpha$ when $p_i \neq p$) as

$$\partial_x\alpha = \alpha(1-\alpha)\partial_x \ln\left(\frac{\alpha}{1-\alpha}\right). \tag{3.27}$$

Indeed we have observed that, when α ($\alpha = \alpha_v$, $1 - \alpha = \alpha_l$) is very small (say 10^{-6}), all the terms in the vapor phase equations almost vanish, but not $\partial_x\alpha$ and this creates instabilities. This also appears for α close to 1 for the liquid phase equations. With the interpretation (3.27) of $p\partial_x\alpha$ (or $p_i\partial_x\alpha$) we get rid of this. Next, it remains to discretize (3.27). The physical quantities appearing in (3.27) will be taken at time t^n. Let

$$\beta_j = \ln\left(\frac{\alpha_j}{1-\alpha_j}\right). \tag{3.28}$$

We will discuss here two cases.

Case 1. $p_i \neq p$. In this case, $p\partial_x\alpha$ is replaced by $p_i\partial_x\alpha = (p - (p - p_i))\partial_x\alpha$ in (3.1) (see (2.1)). The expression of $(p - p_i)$ [2] is given by

$$p - p_i = \xi\rho_c(u_v - u_l)^2, \tag{3.29}$$

where ξ is a constant and ρ_c is the continuous phase density. Other expressions can be found in the literature (see [16, 21]). Here we have used $\xi = 1$ and $\rho_c = \rho_v$. Notice that, in practical tests, the resulting expression is very small numerically.

Case 2. $p_i = p$. The space discretization is different in the two cases. In Case 1, we use the centered formula,

$$(p_i\partial_x\alpha)_j = (p_i)_j\alpha_j(1-\alpha_j)\frac{1}{2\,\Delta x}\{\beta_{j+1} - \beta_{j-1}\}. \tag{3.30}$$

But in Case 2, we use the more stable formula,

$$(p\,\partial_x\alpha)_j = p_j\alpha_j(1-\alpha_j)\frac{1}{\Delta x}\,\mathrm{Minmod}(\beta_{j+1} - \beta_j, \beta_j - \beta_{j-1}), \tag{3.31}$$

where the Minmod function is defined by

$$\mathrm{Minmod}(a, b) = \tfrac{1}{2}(\mathrm{sgn}(a) + \mathrm{sgn}(b))\min(|a|, |b|).$$

In the Case 1, we could have used the Minmod, instead of the centered formula (3.30). We prefer the centered formula which gives sharper fronts. This is possible because the formula (3.29) brings more stability (hyperbolicity) to the continuous system, compared to the case $p_i = p$.

Finally, the quantities computed from this first step are m_k, $m_k u_k$, and E_k ($k = v, l$). These quantities will be identified using the superscript $n + 1/2$.

3.3. *Discretization of the Second Step*

Next, it remains to discretize the two following coupled systems:

$$\begin{cases} \partial_t m_v = 0, \\ \partial_t m_v u_v = 0, \\ \partial_t E_v = -p\,\partial_t\alpha_v, \end{cases} \quad \text{and} \quad \begin{cases} \partial_t m_l = 0, \\ \partial_t m_l u_l = 0, \\ \partial_t E_l = -p\,\partial_t\alpha_l. \end{cases} \tag{3.32}$$

This step can be performed cell by cell and thus we skip the index j throughout this subsection. To ensure stability, we will use an implicit method. First, we remark that the first two equations in each system can be omitted because they only mean that the quantities they involve are time invariant, i.e.,

$$\begin{cases} m_v^{n+1} = m_v^{n+1/2}, \\ (m_v u_v)^{n+1} = (m_v u_v)^{n+1/2}, \end{cases} \text{and} \quad \begin{cases} m_l^{n+1} = m_l^{n+1/2}, \\ (m_l u_l)^{n+1} = (m_l u_l)^{n+1/2}. \end{cases} \tag{3.33}$$

Thus we are reduced to studying

$$\begin{aligned} \partial_t E_v &= -p\,\partial_t\alpha_v, \\ \partial_t E_l &= -p\,\partial_t\alpha_l. \end{aligned} \tag{3.34}$$

We make some further simplifications before stating the ultimate system to be discretized. Recall that

$$E_k = \frac{(m_k u_k)^2}{2m_k} + m_k e_k, \quad k = v, l.$$

By using the equalities (3.33), the system (3.34) amounts to

$$\begin{aligned} \partial_t(m_v e_v) &= -p\,\partial_t\alpha_v, \\ \partial_t(m_l e_l) &= -p\,\partial_t\alpha_l. \end{aligned} \tag{3.35}$$

Adding up the two equations of (3.35) each one (in view of (2.2)) gives

$$\partial_t(m_v e_v) + \partial_t(m_l e_l) = 0. \tag{3.36}$$

To keep this fundamental conservation law, we discretize it as

$$(m_v e_v)^{n+1} + (m_l e_l)^{n+1} = (m_v e_v)^{n+1/2} + (m_l e_l)^{n+1/2}. \tag{3.37}$$

Next, using the relationship

$$\tilde{p}_k = (\gamma_k - 1)m_k e_k, \quad k = v, l, \tag{3.38}$$

the terms in the left-hand side of (3.37); i.e., $(m_k e_k)^{n+1}$ for $k = v, l$, are replaced by $(\alpha_k^{n+1}p^{n+1})/(\gamma_k - 1)$. An easy computation shows that

$$p^{n+1} = \frac{(m_v e_v)^{n+1/2} + (m_l e_l)^{n+1/2}}{\alpha^{n+1}/(\gamma_v - 1) + (1 - \alpha^{n+1})/(\gamma_l - 1)}, \tag{3.39}$$

where $\alpha = \alpha_v$ and $(1 - \alpha) = \alpha_l$.

The unknowns are p and α. To compute them, we need to state another equation; thus, consider the discretized form of the first equation of (3.35)

$$(m_v e_v)^{n+1} - (m_v e_v)^{n+1/2} = -p^{n+1}(\alpha^{n+1} - \tilde{\alpha}). \tag{3.40}$$

The value $\tilde{\alpha}$ should be chosen at time $t^{n+1/2}$, i.e. $\tilde{\alpha} = \alpha^{n+1/2}$, and then the system (2.1) would be solved in two fractional steps. Now, $\alpha^{n+1/2}$ is unknown from the first step, since the computed variable is $m_v^{n+1/2} = \alpha^{n+1/2}\rho_v^{n+1/2}$ and from this relationship we cannot deduce $\alpha^{n+1/2}$. For this reason, we set $\tilde{\alpha} = \alpha^n$ and, as a consequence, the system (2.1) is solved in a *single step*. (To check this, add the discretized systems of (3.1) (for $k = v, l$) to those of (3.3) (for $k = v, l$)). We now have

$$(m_v e_v)^{n+1} - (m_v e_v)^{n+1/2} = -p^{n+1}(\alpha^{n+1} - \alpha^n). \tag{3.41}$$

Using (3.38), we get after some algebraic manipulations

$$p^{n+1} = m_v^{n+1/2} e_v^{n+1/2}\left(\frac{\gamma_v \alpha^{n+1}}{(\gamma_v - 1)} - \alpha^n\right)^{-1}. \tag{3.42}$$

Finally, replacing p^{n+1} in (3.39) by its expression in (3.42) yields an equation with the unique unknown α^{n+1}. Some tedious calculations give the explicit expression

$$\alpha^{n+1} = \frac{(1/(\gamma_l - 1) + \alpha^n)m_v^{n+1/2}e_v^{n+1/2} + \alpha^n m_l^{n+1/2}e_l^{n+1/2}}{(\gamma_l/\gamma_l - 1)m_v^{n+1/2}e_v^{n+1/2} + (\gamma_v/(\gamma_v - 1))m_l^{n+1/2}e_l^{n+1/2}}. \tag{3.43}$$

Notice that although it does not seem to be, this expression is indeed symmetric with respect to the two phases. Next, the explicit expression of p^{n+1} is obtained plugging α^{n+1}, given by (3.43), into (3.39).

We are now in a position to update all the main variables involved in the system of equations, i.e. α, p, m_v, $m_v u_v$, E_v, m_l, $m_l u_l$, E_l and the variables involved in their expressions, i.e. $(\rho_k, u_k, e_k, k = v, l)$.

4. PROPERTIES OF THE METHOD WHEN BASED ON KINETIC SCHEMES

In this section, we give several theoretical properties of the method based on the kinetic scheme in Case 2, where the Minmod discretization (3.31) of the term $p\,\partial_x\alpha$ was introduced to make up the lack of hyperbolicity. The hyperbolic case (Case 1) is not addressed here but strong numerical evidence assessed its stability properties.

This method preserves several basic properties of the initial system. By using the finite-volume method and the conservative variables for the computed unknowns, we have conservation of total mass, momentum, and energy. We strengthen at first (3.23), setting

$$\Delta t \le \Delta x/2(|u_j^n| + \sqrt{3}\,\sqrt{\tilde{p}_j^n/m_j^n}). \tag{4.1}$$

The weak stability result is given by the following.

THEOREM 1. *Suppose that at the time level t^n, we have $\rho_k^n \ge 0$ for $k = v, l$; $p^n \ge 0$ and $0 < \alpha_k^n < 1$. Then, we get $\rho_k^{n+1} \ge 0$, $p^{n+1} \ge 0$ and $0 < \alpha_k^{n+1} < 1$ under the CFL conditions* (4.1) *and* (4.2) (*see the notations in the proof below*)

$$\frac{\Delta t}{\Delta x}\max_{j,k}\frac{1}{\lambda_k}|\Delta\beta_j^n|\,|u_{kj}^{n+1/2}| \le \frac{1}{2}, \tag{4.2}$$

which is also implied by the condition acting only at time level n:

$$\frac{\Delta t}{\Delta x}\max_{j,k}\frac{1}{\lambda_k}|\Delta\beta_j^n|\left(|u_{kj}^n| + \frac{\Delta t}{\Delta x}M_{kj}^n\right) \le \frac{1}{4}. \tag{4.3}$$

Remarks. 1. These estimates are crude, but give a time-step of the order of the usual CFL condition. They guarantee that α remains in $]0, 1[$. The time-step could become very small (as in usual monophasic gas dynamics) but in practice this does not occur as we shall see even in the separation problem (Section 5, Problem 1).

2. To the best of our knowledge these positivity results are new and are directly inherited from the splitting method we have proposed.

3. $\Delta\beta_j^n$ is given by (see 3.31)

$$\Delta\beta_j^n = \text{Minmod}\left(\ln\left(\frac{\alpha_{j+1}^n(1-\alpha_j^n)}{\alpha_j^n(1-\alpha_{j+1}^n)}\right), \times \ln\left(\frac{\alpha_j^n(1-\alpha_{j-1}^n)}{\alpha_{j-1}^n(1-\alpha_j^n)}\right)\right). \tag{4.4}$$

Proof of Theorem 1. We consider the phase associated, for instance, with the void fraction α. We know that $f(x, v, t^n)$ and $g(x, v, t^n)$ are nonnegative functions. Since they solve transport equations we also have $f(x, v, t^{n+1/2}) \geq 0$ and $g(x, v, t^{n+1/2}) \geq 0$. And thus,

$$m_j^{n+1/2} = \frac{1}{\Delta x}\int_{\mathbb{R}\times K_j} f(x, v, t^{n+1/2})\, dv\, dx \geq 0. \tag{4.5}$$

We write

$$\begin{aligned} E_j^{n+1/2} &= m_j^{n+1/2}\left(\frac{1}{2}(u_j^{n+1/2})^2 + e_j^{n+1/2}\right) \\ &= \frac{1}{\Delta x}\int_{\mathbb{R}\times K_j}\left[\frac{v^2}{2} f(x, v, t^{n+1/2}) + g(x, v, t^{n+1/2})\right] dv\, dx \\ &= \frac{1}{\Delta x}\int_{\mathbb{R}\times K_j}\frac{1}{2}(v - u_j^{n+1/2})^2 f(x, v, t^{n+1/2}) \\ &\quad - \frac{1}{2} m_j^{n+1/2}(u_j^{n+1/2})^2 \\ &\quad + (u_j^{n+1/2})\frac{1}{\Delta x}\int_{\mathbb{R}\times K_j} v f(x, v, t^{n+1/2}) \\ &\quad + \frac{1}{\Delta x}\int_{\mathbb{R}\times K_j} g(x, v, t^{n+1/2})\, dv\, dx. \end{aligned}$$

Now, following (3.5) and (3.20) we have

$$\begin{aligned} &\frac{1}{\Delta x}\int_{\mathbb{R}\times K_j} v f(x, v, t^{n+1/2})\, dx\, dv \\ &\qquad = m_j^{n+1/2} u_j^{n+1/2} - \frac{\Delta t}{\Delta x} p_j^n\, \Delta\alpha_j^n, \end{aligned} \tag{4.6}$$

where $p_j^n(\Delta\alpha_j^n/\Delta x)$ is the discretization associated with $p\,\partial_x\alpha$. This yields

$$\begin{aligned} &m_j^{n+1/2} e_j^{n+1/2} + u_j^{n+1/2}\frac{\Delta t}{\Delta x} p_j^n\, \Delta\alpha_j^n \\ &\qquad = \frac{1}{\Delta x}\int_{\mathbb{R}\times K_j}\frac{1}{2}(v - u_j^{n+1/2})^2 f(x, v, t^{n+1/2}) \\ &\qquad\quad + \frac{1}{\Delta x}\int_{\mathbb{R}\times K_j} g(x, v, t^{n+1/2})\, dv\, dx. \end{aligned} \tag{4.7}$$

The condition (4.1) implies that $|v|(\Delta t/\Delta x) \leq \frac{1}{2}$ and, after integration of $f(x, v, t^{n+1/2}) = f^n(x - v\Delta t, v)$ and $g(x, v, t^{n+1/2}) = g^n(x - v\Delta t, v)$ over $\mathbb{R}\times K_j$, we obtain after some tedious but easy calculations

$$m_j^{n+1/2} \geq \tfrac{1}{2} m_j^n > 0, \tag{4.8}$$

and furthermore,

$$\int_{\mathbb{R}\times K_j} g(x, v, t^{n+1/2})\, dv\, dx \geq \frac{1}{2}\lambda\alpha_j^n p_j^n. \tag{4.9}$$

Therefore, using (4.9) we get from (4.7):

$$m_j^{n+1/2} e_j^{n+1/2} \geq \frac{1}{2}\lambda\alpha_j^n p_j^n - \frac{\Delta t}{\Delta x} p_j^n\, \Delta\alpha_j^n u_j^{n+1/2}. \tag{4.10}$$

Notice that $p\,\partial_x\alpha$ has been transformed into $p\alpha(1-\alpha)\partial_x\beta$ (see (3.27)), with $\beta = \ln(\alpha/(1-\alpha))$. Denoting $\Delta\beta_j^n/\Delta x$ the discretization associated with $\partial_x\beta$, the inequality (4.10) reduces to

$$\begin{aligned} m_j^{n+1/2} e_j^{n+1/2} &\geq \alpha_j^n p_j^n \\ &\quad \times\left(\frac{1}{2}\lambda - \frac{\Delta t}{\Delta x}(1-\alpha_j^n)\,\Delta\beta_j^n u_j^{n+1/2}\right). \end{aligned} \tag{4.11}$$

In practice, the velocity $|u_j^{n+1/2}|$ is a finite quantity and the condition (4.2) is sufficient to ensure (see (4.7))

$$e_j^{n+1/2} \geq 0. \tag{4.12}$$

Now, we have proved that the variables $m_k^{n+1/2}$ and $e_k^{n+1/2}$ are nonnegative.

Since $\gamma_l > 1$, $\gamma_v > 1$, and $0 < \alpha^n < 1$, we have

$$0 < \frac{1}{\gamma_l - 1} + \alpha^n < \frac{\gamma_l}{\gamma_l - 1}, \quad 0 < \alpha^n < \frac{\gamma_v}{\gamma_v - 1}, \tag{4.13}$$

this implies that

$$\begin{aligned} 0 &< \left(\frac{1}{\gamma_l - 1} + \alpha^n\right) m_v^{n+1/2} e_v^{n+1/2} + \alpha^n m_l^{n+1/2} e_l^{n+1/2} \\ &< \frac{\gamma_l}{\gamma_l - 1} m_v^{n+1/2} e_v^{n+1/2} + \frac{\gamma_v}{\gamma_v - 1} m_l^{n+1/2} e_l^{n+1/2} \end{aligned} \tag{4.14}$$

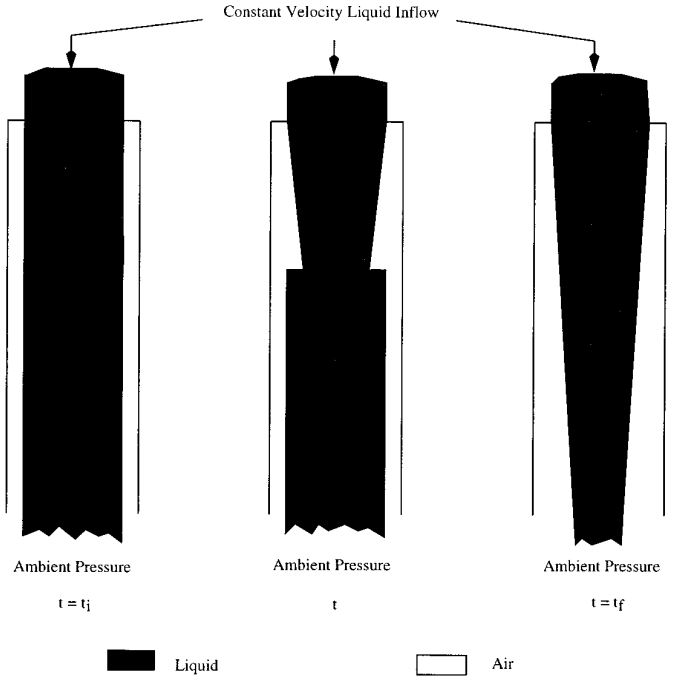

FIG. 1. Water faucet problem evolution.

Using (3.43), it follows that

$$0 < \alpha^{n+1} < 1. \tag{4.15}$$

Following (4.15) and (3.39) we get

$$p^{n+1} \geq 0. \tag{4.16}$$

Finally, (3.33) and (4.15) give

$$\rho_k^{n+1} \geq 0 \quad (k = v, l). \tag{4.17}$$

Hence, we have proved the result under the condition (4.2).

Now, we will attempt to upperbound $|u_j^{n+1/2}|$ in order to recover (4.3). We argue as follows:

$$\begin{aligned}\frac{1}{\Delta x}\int_{\mathbb{R}\times K_j} v f(x, v, t^{n+1/2})\, dx\, dv \\ = m_j^n u_j^n + \frac{\Delta t}{\Delta x}\left[\int_{v\geq 0} v^2 f_{j-1}(v)\, dv - \int_{v\geq 0} v^2 f_j(v)\, dv\right. \\ \left. + \int_{v\leq 0} v^2 f_j(v)\, dv - \int_{v\leq 0} v^2 f_{j+1}(v)\, dv\right].\end{aligned} \tag{4.18}$$

Following (4.6) and (4.18), we obtain

$$\begin{aligned}m_j^{n+1/2} u_j^{n+1/2} = m_j^n u_j^n \\ + \frac{\Delta t}{\Delta x}\left[\int_{v\geq 0} v^2 (f_{j-1}(v) - f_j(v))\, dv\right. \\ \left. + \int_{v\leq 0} v^2 (f_j(v) - f_{j+1}(v))\, dv\right] \\ - \frac{\Delta t}{\Delta x} p_j^n\, \Delta\alpha_j^n,\end{aligned} \tag{4.19}$$

and we have only to consider the case where $u_j^{n+1/2}$ and $\Delta\alpha_j^n$ have the same sign, say nonnegative. Then

$$\begin{aligned}m_j^{n+1/2} u_j^{n+1/2} \leq m_j^n u_j^n + \frac{\Delta t}{\Delta x}\left[\int_{v\geq 0} v^2 f_{j-1}(v)\, dv\right. \\ \left. + \int_{v\leq 0} v^2 f_j(v)\, dv\right]\end{aligned} \tag{4.20}$$

and, using (4.8), we have

$$u_j^{n+1/2} \leq 2\left(|u_j^n| + \frac{\Delta t}{\Delta x}\frac{\tilde{M}_j^n}{m_j^n}\right), \tag{4.21}$$

with

$$\begin{aligned}\tilde{M}_j^n = \max\left(\int_v v^2 (f_{j-1}(v)\right. \\ \left. + f_j(v))\, dv, \int_v v^2 (f_{j+1}(v) + f_j(v))\, dv\right) \\ = m_j^n (|u_j^n|^2 + e_j^n) \\ + \max_j (m_{j-1}^n (|u_{j-1}^n|^2 + e_{j-1}^n), m_{j+1}^n (|u_{j+1}^n|^2 + e_{j+1}^n)).\end{aligned} \tag{4.22}$$

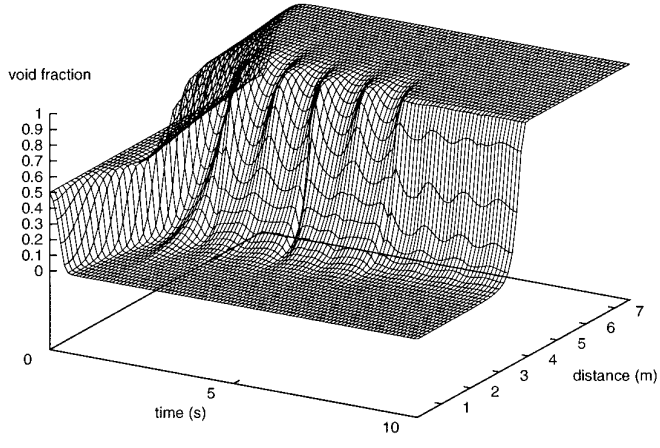

FIG. 2. Void fraction in space-time plane (Case 1), 50 cells.

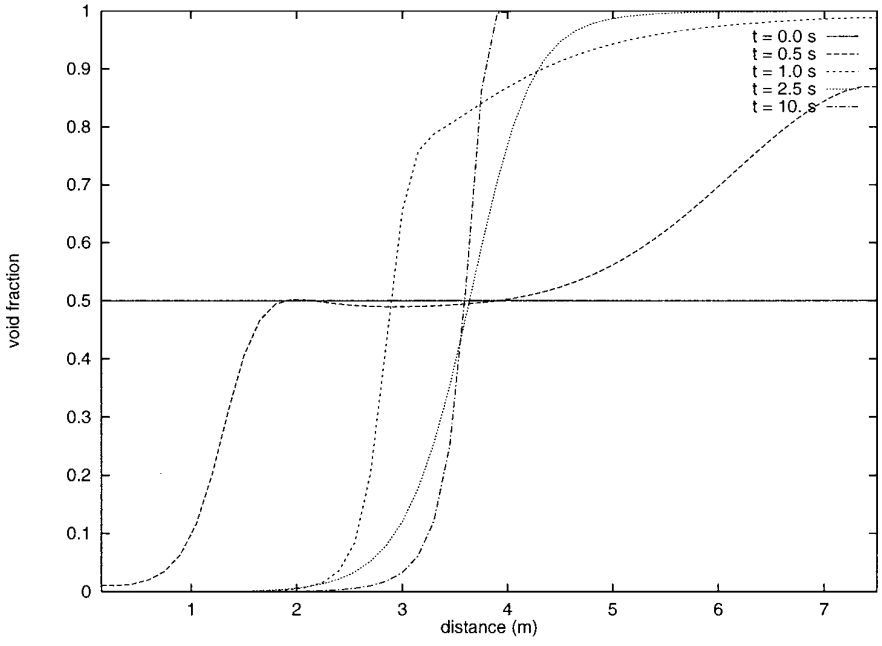

FIG. 3. Void fraction history, 50 cells.

In this formula, the "max" comes from the necessity to consider also the other possibility when $u_j^{n+1/2}$ and $\Delta\alpha_j^n$ are negative.

We can rewrite (4.21) as

$$|u_j^{n+1/2}| \le 2\left(|u_j^n| + \frac{\Delta t}{\Delta x} M_j^n\right), \tag{4.23}$$

with

$$M_j^n = \tilde{M}_j^n / m_j^n. \tag{4.24}$$

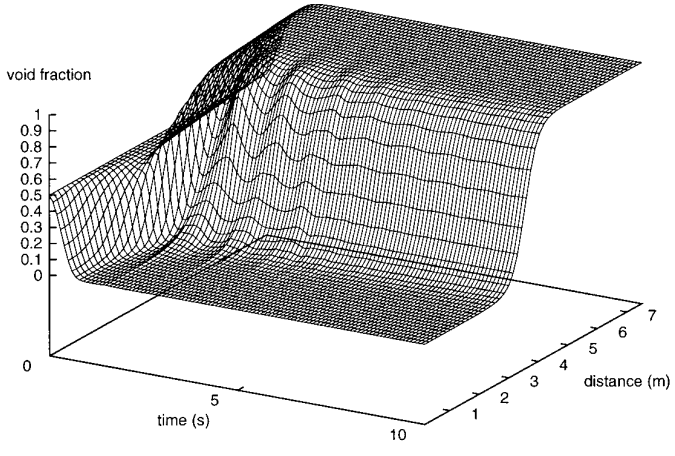

FIG. 4. Void fraction in space-time plane (Case 2), 50 cells.

5. NUMERICAL RESULTS

Problem 1: *Sedimentation*

This problem represents a very simplified physical phenomena: separation of air and water by gravity in a vertical tube. The objective of this problem is to check the capability of the model and of the chosen numerical approach to describe countercurrent flow conditions and the occurrence of strong void gradients which are typical of many situations where phase separation phenomena are dominating.

The test consists of a vertical tube of 7.5 m length. In the initial state, the tube is filled with a homogeneous two-phase mixture (air, water) of constant void fraction of $\alpha = 0.5$; the velocities are $u_v = u_l = 0$ m/s. The boundary conditions at the inlet and the outlet are nul debits for the vapor and the liquid; i.e., the velocities of the two fluids are forced to equal zero at the two ends of the duct, since these are closed. The phase separation is due to gravity forces only. The liquid phase falls down to the bottom of the tube, while the gas phase comes up to the top of the tube.

All the presented results have been achieved using a constant ratio $\Delta t/\Delta x = 6.0E - 4$. Figures 2 and 4 below show in the space-time plane the predicted values for the void fraction in Case 1 and Case 2 (i.e., $p_i \neq p$ and $p_i = p$). The comparison between the steady-state solution for the two cases is given in Fig. 5, this figure clearly indicates that the steady-state solution in Case 1 is much closer

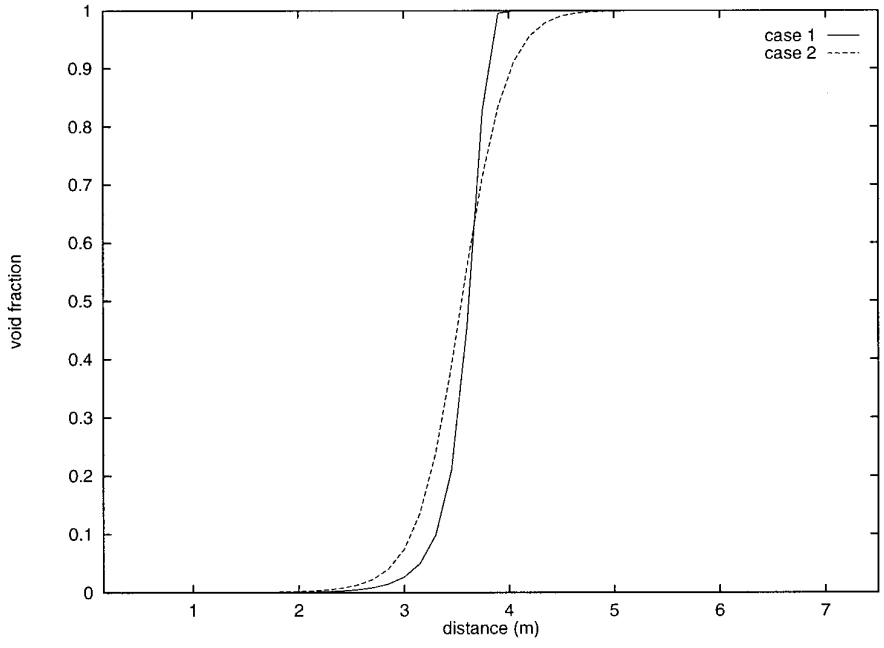

FIG. 5. Comparison between steady-state solutions, t = 10 s, 50 cells.

to the expected analytical steady-state solution than in Case 2.

The void fraction distribution along the vertical height at different time levels is shown in Fig. 3, this figure indicates an upward and downward directed void front in the transient period; the occurrence of quasi-stationary conditions is achieved once the two fronts have merged at the middle section of the tube.

Figure 6 shows the spatial convergence of the void fraction at the steady-state. We give below the errors

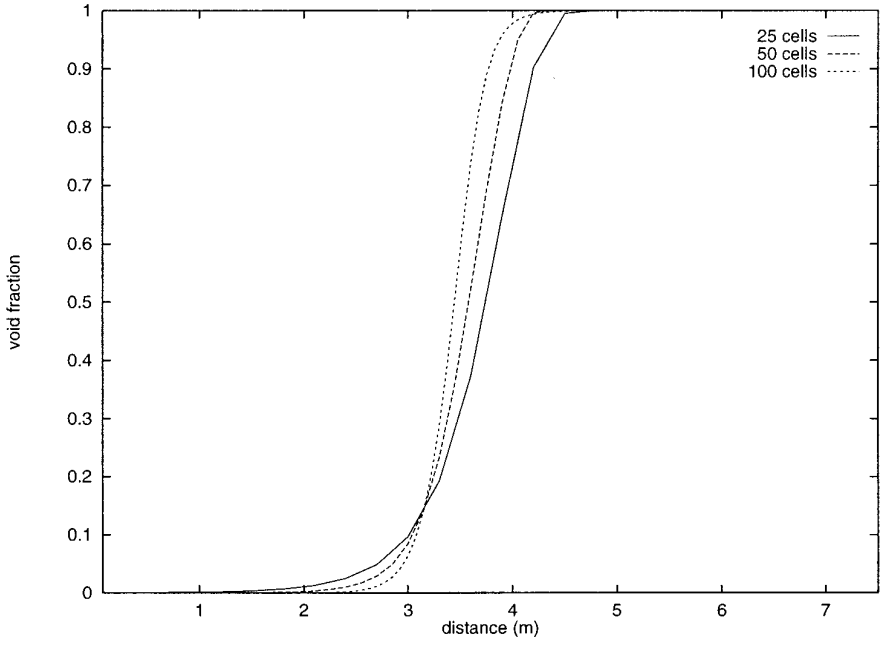

FIG. 6. Spatial convergence of steady-state solution (Case 1), t = 6.5 s.

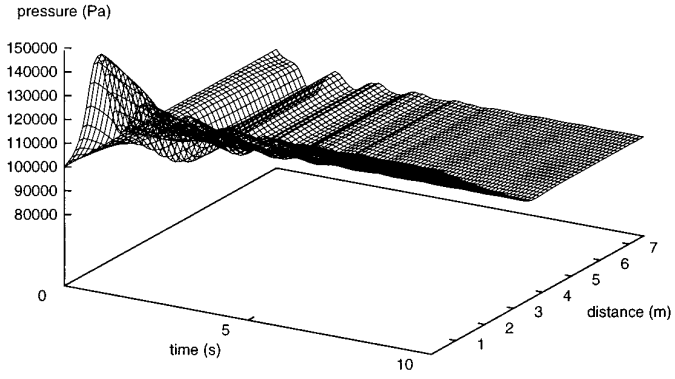

FIG. 7. Pressure in space-time plane (Case 2), 50 cells.

in L^1 norm, choosing the finest grid solution as the reference one.

Error_1	Error_2	θ
0.2090	0.1069	0.9662

Where $\text{error}_1 = \|\alpha_{25} - \alpha_{100}\|_1$ and $\text{error}_2 = \|\alpha_{50} - \alpha_{100}\|_1$, the subscripts represent the number of cells. Here $\theta = \log(\text{error}_1/\text{error}_2)/\log(h_1/h_2)$ provides an estimate of the order of accuracy ($h_1 = 7.5/25$ and $h_2 = 7.5/50$).

Figure 7 shows the predicted values for the pressure in space-time plane in Case 2. One can notice the establishment of a static pressure gradient in the gas and liquid regions. Figure 8 compares the steady pressure profiles in Cases 1 and 2. Not only does Case 1, because of the centered discretization, give an overshoot, as can be seen in Fig. 8, but also it is very sensitive to the number of computational cells. These results can be compared to those obtained by [18].

Problem 2: *Water Faucet*

The water faucet problem (see [13]) consists of a vertical tube 12 m in length and 1 m in diameter. The top has a fixed inflow rate of water at a velocity of 10 m/s, temperature of 50°C, and a liquid volume fraction of 0.8. The bottom of the tube is open to the ambiant pressure and the top of the tube is closed to vapor flow. The problem is illustrated schematically in Fig. 1.

Initially, the tube is filled with a uniform column of water at a velocity of 10 m/s surrounded by stagnant vapor, such that the vapor volume fraction is 0.2. The thermodynamic properties of the system at the initial state are assumed constant at values appropriate for air–water mixture and are 50°C for the temperature and 10^5 (Pascal) for the pressure.

The velocity boundary conditions at the inlet are 10 m/s for the liquid and 0.0 m/s for the vapor. The volume fraction of the vapor at the inlet is set constant at 0.2. The only outflow boundary condition at the bottom of the tube is constant pressure at 10^5 (Pascal). These specific boundary conditions are implemented using the solution

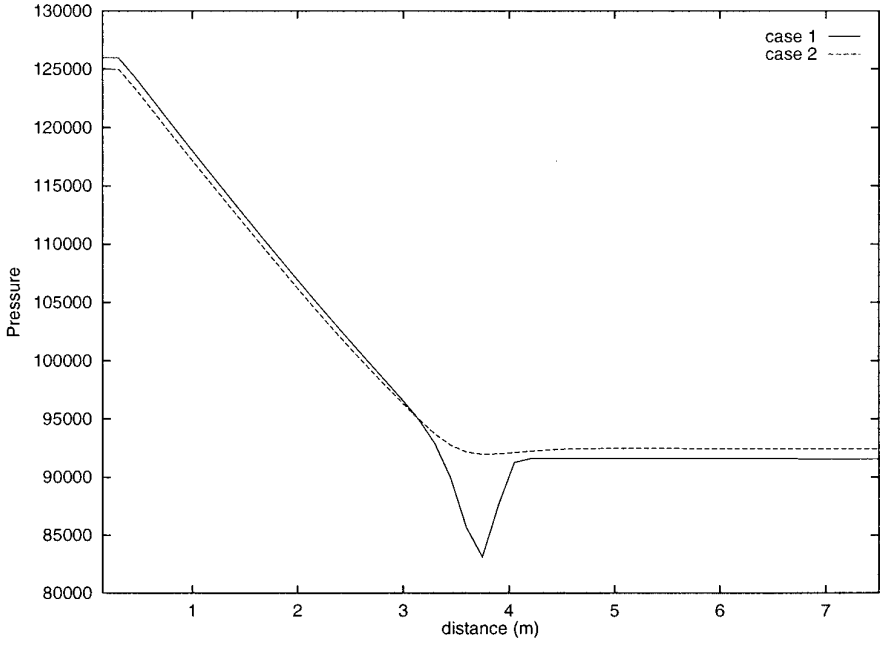

FIG. 8. Comparison between steady-state solutions, t = 10 s, 50 cells.

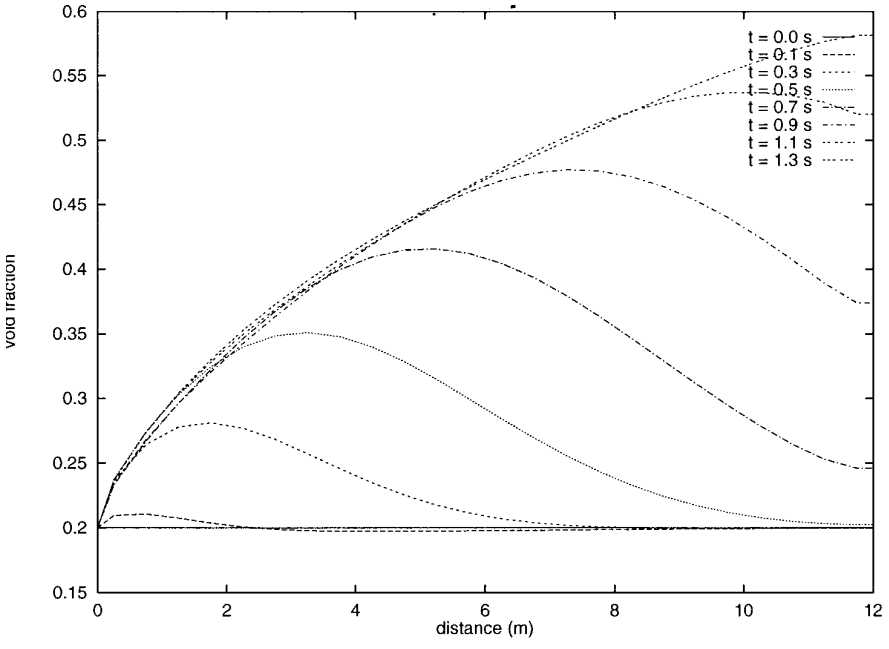

FIG. 9. Transient void fraction profile, 24 cells.

of a half-Riemann problem which is described in detail in [1]. Here, for physical considerations (see [13]), we are led to choose $p_i = p$. The calculation is carried out until a steady flow is attained. This transient problem has a particularly simple analytical solution when pressure variation in the vapor (and, hence, in the liquid) is ignored (see [13]). This analytical solution was used as a code test problem in [14]. The objective of this problem is to test the stability and the convergence of the numerical solution method. The diffusive character of the numerical method is also tested since a discontinuity in the void fraction is propagated through the solution space.

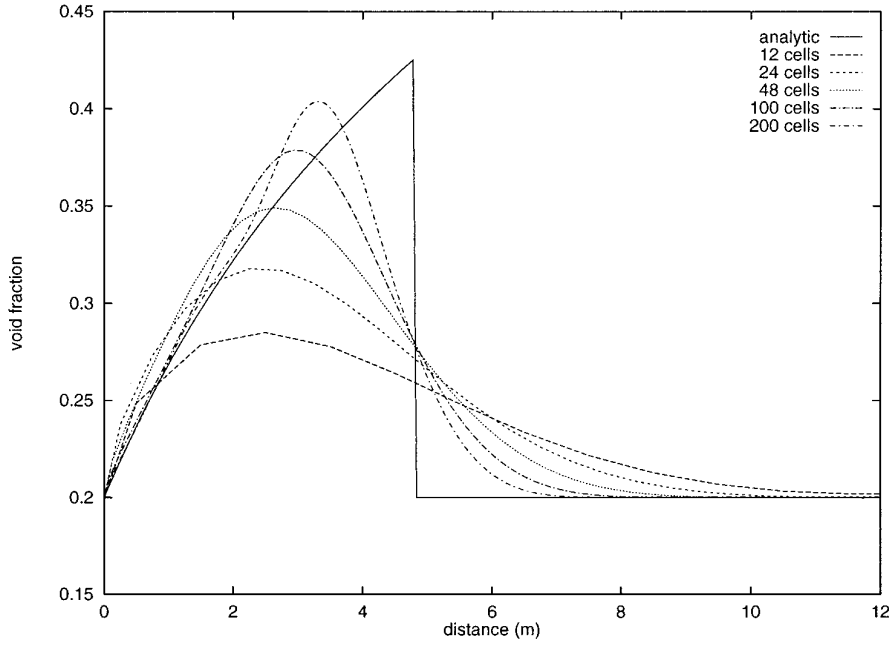

FIG. 10. Convergence void fraction profile, t = 0.4 s.

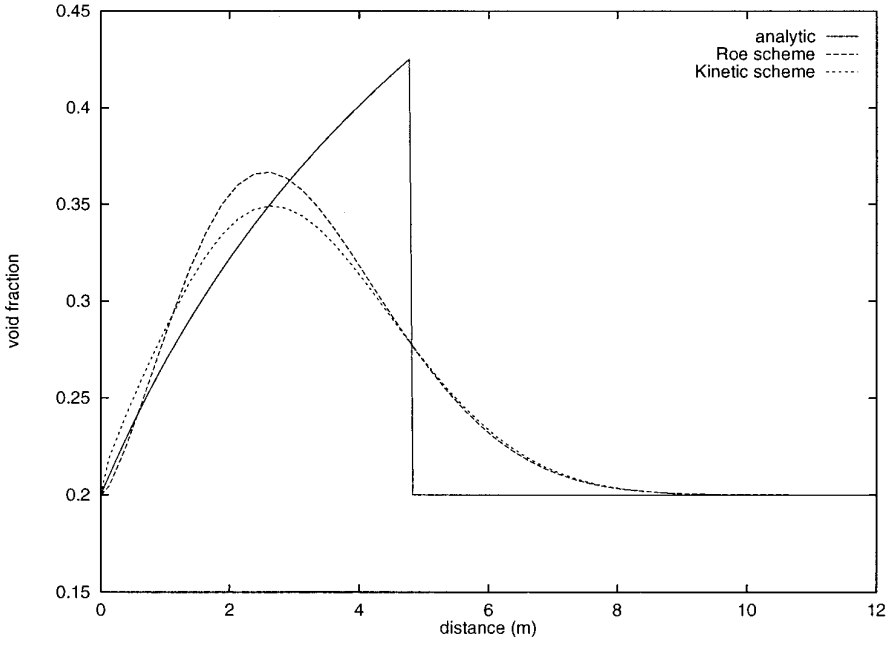

FIG. 11. Convergence void fraction profile, t = 0.4 s, 48 cells.

All the computations have been achieved using a constant ratio $\Delta t/\Delta x = 5.0E - 4$. The void fraction as a function of space at different times is shown in Fig. 9. This figure shows the dynamic propagation of the void profile down the tube until the wave has completely passed out of the tube and the steady-state profile remains.

In order to check the convergence and the stability of the scheme, computations have been made using a discreti-

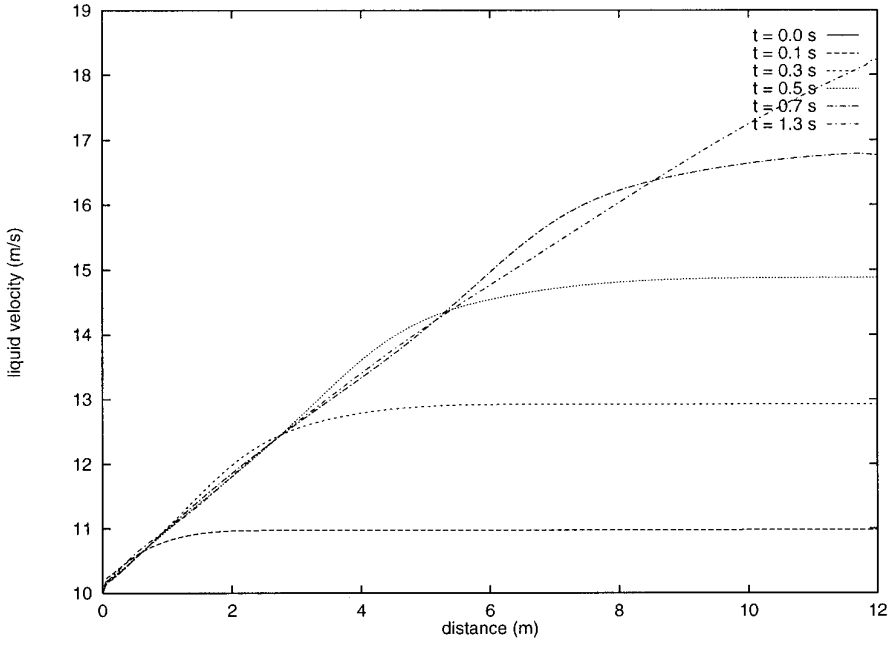

FIG. 12. Transient liquid velocity profile, 96 cells.

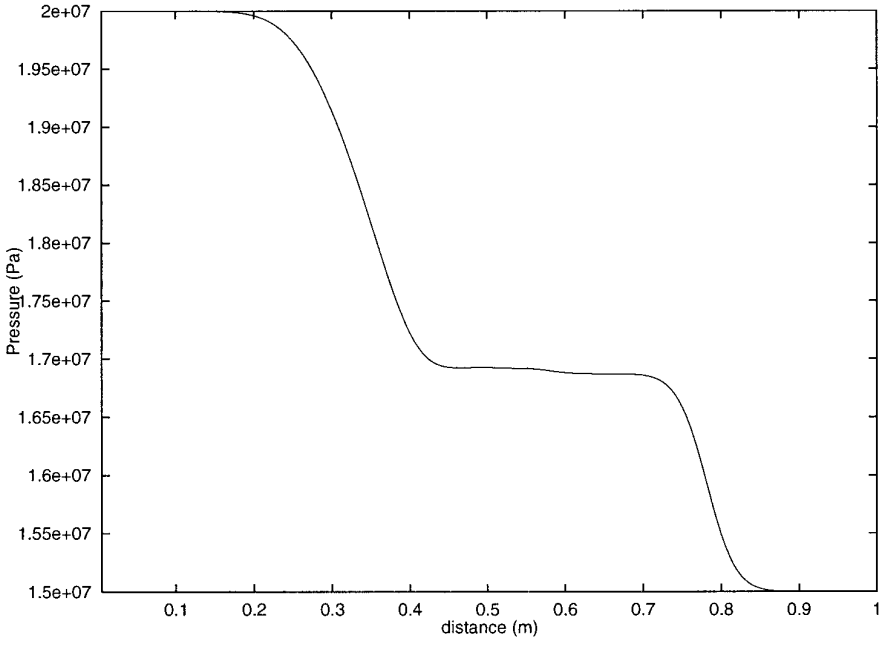

FIG. 13. Pressure profile.

zation with 12, 24, 48, 100, and 200 cells. The void fraction profiles for various discretisations are compared to the above-mentioned analytical solution (see Fig. 10), which is explicitly given by

$$\alpha(x,t) = \begin{cases} 1 - \dfrac{\alpha_l^e u_l^e}{\sqrt{2gx + (u_l^e)^2}}, & \text{if } x \le u_l^e t + \dfrac{gt^2}{2}, \\ 0.2, & \text{otherwise,} \end{cases} \tag{5.1}$$

where $u_l^e = 10$ m/s and $\alpha_l^e = 0.8$.

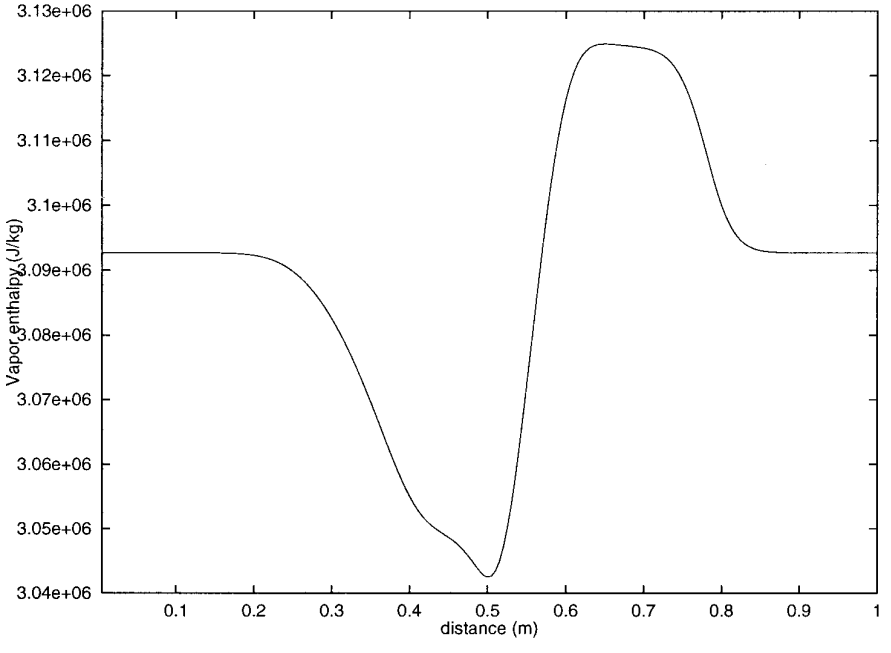

FIG. 14. Vapor enthalpy profile.

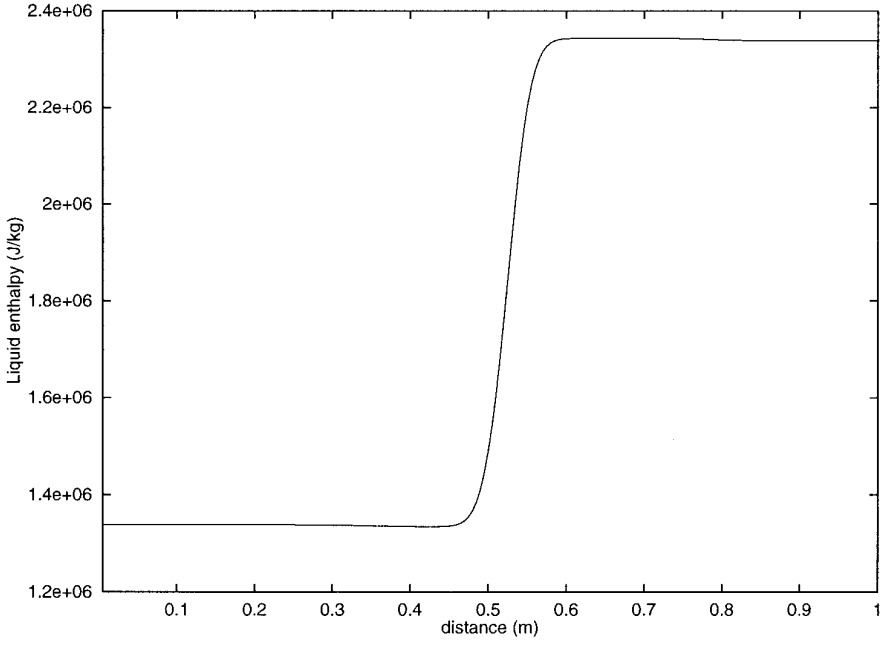

FIG. 15. Liquid enthalpy profile.

The L^1 norm errors between the approximate and analytical solutions are displayed in the following table:

Error_1	Error_2	Error_3	Error_4	Error_5	θ
0.4761	0.3796	0.2793	0.2141	0.1674	0.3717

with $\text{error}_i = \|\alpha_i - \alpha_{\text{analytical}}\|$ and i refers to the various discretizations ($i = 1$ for 12 cells, $i = 2$ for 24 and so on). Here θ denotes an average value of the $\theta_i = \log(\text{error}_{i-1}/\text{error}_i)/\log(h_{i-1}/h_i)$.

We compare in the Fig. 11 the profile given by the kinetic and Roe solvers in the first step. As announced, the Roe solver is more accurate. Finally, the transient liquid velocity profile is given in Fig. 12.

Problem 3: *Shock Tube Problem*

In order to show that the algorithm is able to handle large differences between liquid and gas (vapor) temperatures, we present a two-phase shock tube problem. The initial data is given by the following table:

	α	p (bar)	u_v (m/s)	u_l (m/s)	h_v (kj/kg)	h_l (kj/kg)	γ_v	γ_l
U^L	0.25	200.	0.	0.	3092.7	1338.2	1.0924	1.0182
U^R	0.25	150.	0.	0.	3092.7	2338.2	1.0924	1.0182

Notice, however, that the mathematical meaning of this problem with shocks is quite imprecise (see [3]), and there is no physical interpretation for this case because the thermodynamical disequilibrium requires exchange terms between phases. The computations have been achieved using 200 cells and a constant ratio $\Delta t/\Delta x = 5.0E - 4$. In Figs. 13, 14, and 15, we show the pressure and enthalpies profiles at time $t = 0.75E - 03$.

ACKNOWLEDGMENTS

This work has been financially supported by EDF/DER/RNE under Contract T131H8968. The authors thank the referees for their valuable remarks which led to substantial improvement of the first version of this paper.

REFERENCES

1. K. El Amine, Thèse de Doctorat de l'Université Paris **VI,** (1997).
2. K. El Amine and P. Rascle, *Ecoulement Diphasique, Modélisation et Hyperbolicité,* Rapport interne EDF HT-13/96/004, 1996.
3. G. Dal Maso, P. Le Floch, and F. Murat, Definition and weak stability of nonconservative products, *J. Math. Pures Appl.* **74,** 483 (1995).
4. J. M. Ghidaglia, A. Kumbaro, and G. Le Coq, Une méthode volumes finis à flux caractéristiques pour la résolution numérique des systèmes hyperboliques de lois de conservation, *C. R. Acad. Sci. Paris Sér. I* **322,** 981 (1996).
5. E. Godlewski & P.-A. Raviart, Hyperbolic systems of conservation laws, *Ellipses Math. Appl.* **3/4** (1990).
6. E. Godlewski & P.-A. Raviart, *Numerical Approximation of Hyperbolic Systems of Conservation Laws,* Amer. Math. Soc. Vol. 118 (Springer-Verlag, New York, 1996).

7. A. Harten, P. D. Lax, and B. Van Leer, On upstream differencing and Godunov-type schemes for hyperbolic conservation laws, *SIAM Rev.* **25**(1), 35 (1983).
8. G. F. Hewitt, J. M. Delhaye, and N. Zuber, *Multiphase Science and Technology,* Vol. 5 (Hemisphere, Washington, DC/New York, 1990).
9. M. Ishii, *Thermo-Fluid Dynamic Theory of Two-Phase Flow* (Eyrolles, Paris, 1975).
10. R. T. Lahey & D. A. Drew, The three dimensional time and volume averaged conservation equations of two-phase flow, *Adv. Nuc. Sci. Technol.* **20,** 1 (1988).
11. S. Osher & E. Tadmor, On the convergence of difference approximations to scalar conservation laws, *Math. Comp.* **181,** 19 (1988).
12. B. Perthame, Second-order Boltzmann schemes for compressible Euler equations in one and two space dimensions, *SIAM J. Numer. Anal.* **29**(1), 1 (1992).
13. V. H. Ransom, *Numerical Benchmark Tests,* Multiphase Science and Technology, Vol. 3, edited by G. F. Hewitt, J. M. Delhay, and N. Zuber (Hemisphere, Washington, DC, 1987).
14. V. H. Ransom and V. Mousseau, Convergence and accuracy of the Relap5 two-phase flow model, in *Proceedings ANS International Topical Meeting on Advances in Mathematics, Computations and Reactor Physics, Pittsburgh, PA, 1991.*
15. P. L. Roe, Approximate Riemann Solvers, Parameter Vectors, and Difference Schemes, *J. Comput. Phys.* **43,** 357 (1981).
16. L. Sainsaulieu, *Contribution à la modélisation mathématique et numérique des écoulements diphasiques constitués d'un nuage de particules dans un écoulement de gaz,* Thèse d'Habilitation à diriger des recherches, Université Paris **VI,** 1995.
17. A. S.-L. Shieh, R. Krishnamurthy, and V. H. Ransom, Stability, accuracy, and convergence of the numerical methods in RELAP5/MOD3, *Nucl. Sci. Eng.* **116,** 227 (1994).
18. H. Städtke, G. Franchello, and B. Worth, Numerical simulation of multidimensional two-phase flow based on hyperbolic flow equations, [preprint] in *30th Meeting of the European Two-phase Flow Group Piacenza, June 6–8, 1994, Italy*.
19. H. B. Stewart & B. Wendroff, Two-phase flow: Models and methods, *J. Comput. Phys.* **56,** 363 (1984).
20. I. Toumi, A weak formulation of Roe's approximate Riemann solver, *J. Comput. Phys.* **102,** 360 (1992).
21. I. Toumi, *An Upwind Numerical Method for a Six Equation Two-Phase Flow Model,* Rapport DMT/94/168, SERMA/LETR/94/1619, C.E.A., 1994.
22. J. A. Trapp and R. A. Riemke, A nearly-implicit hydrodynamic numerical scheme for two-phase flows, *J. Comput. Phys.* **66,** 62 (1986).
23. G. B. Wallis, *One-Dimensional Two-Phase Flow,* McGraw–Hill, New York, 1969.